

Acknowledgements

First and foremost I would like to thank my supervisor, prof. Henrik Johansson. He was the one who recruited me to the department of Theoretical Physics, and his neverending enthusiasm has kept me going. Other people who have contributed to this work in various ways are Sven Larsson and Per Lincoln, both from the department of Physical Chemistry, and Nina Kann from the department of Organic Chemistry. My thanks also goes to everybody at Theoretical Physics who have answered my questions about computers, opened the door for me when I forgot my key, and generally been good workmates.

Contents

1	Introduction	3
2	The chemistry of DNA	5
2.1	Different types of chemical bonds	5
2.2	DNA bases	6
3	Some basic theory of mesoscopic electronics	11
3.1	The relation between conductance and transmittance	11
3.2	Green's functions	12
3.3	Self energy for a two dimensional metal lead	14
3.4	The Fisher-Lee-relation	14
4	Tight-binding models for DNA	16
4.1	Generic tight-binding model	16
4.2	The two-channel tunneling model	17
4.3	Parameters	18
5	Calculations and results	19
5.1	A 30 base-pair poly(dG) molecule	19
5.2	Random DNA: 30 base-pairs from <i>avena sativa</i>	21
A	The Matlab code used	27
A.1	Generic tight-binding model	27
A.2	The two-channel model	29
	References	32

Chapter 1

Introduction

The basic structure of DNA is well known: a double helix consisting of two strands. Each strand has a backbone built from sugar and phosphate, to which the bases are attached. There are four different bases: adenine, cytosine, guanine and thymine, mostly denoted by their initials. G and C can associate, forming three hydrogen bonds, and similarly A and T bind together via two hydrogen bonds. In this manner the strands combine to form the double helix.

In the helix, the aromatic DNA bases are stacked much like in an aromatic crystal. Because some such crystals are conducting, it has long been hypothesized that DNA might be a conductor as well. [1] Its unique recognition and self-assembly properties could then be used for bottom-up designs of electronic circuits in the nanometre range. Another possible application is the DNA chip, used for DNA sequencing, disease screening, and gene expression analysis. Currently, these chips are read optically. If the conduction properties of DNA turn out to be right, the chips could be read electronically, and hence made faster and more compact. [2]

In the past decade, several experiments have been performed, with conflicting results. DNA has been studied both in its native aqueous solution, and under dry conditions. Since my calculations assume that the piece of DNA is suspended in vacuum between metal electrodes, I will only relate the experiments on dry DNA.

In 1999, Fink and Schönenberger reported the first conductance measurements on DNA bundles in vacuum. [3] They used DNA from the λ phage, and found the molecule to be a metallic conductor. Soon after, Porath *et al* published their results: that a DNA molecule with only GC base pairs is a wide-bandgap semiconductor. [4] Most subsequent publications seem to agree that DNA is indeed semiconducting ([5],[6],[7]) but there has also been groups who have reported isolating behaviour ([8], [9]), and even proximity-

induced superconduction ([10]).

Several things add to the complicated state of this matter. Foremost is the variability of the DNA molecule itself. Apart from different base sequences, this huge molecule has many conformations to choose from, with different alignment of the bases, and different distance between them. Another factor, difficult to control and not very well understood, is the contact between the molecule and the electrodes. A computational study by Tada *et al.* [11] finds that if the DNA is coupled to the leads via the sugar-phosphate backbone, the conductance is seven orders of magnitude less than if the contact is made via the bases, showing the importance of controlling this contact carefully. Also, the method of depositing the DNA for the experiment can seriously affect the delocalization of injected charges, and hence the conductance. This has been studied by Heim *et al.* [12].

Chapter 2

The chemistry of DNA

2.1 Different types of chemical bonds

A basic result of quantum physics is that an electron in an atom is confined to having a certain energy and being in a certain region in space. The electron is said to occupy an orbital. There can be only two electrons in a given orbital, and they must have opposite spins. Orbitals are classified into shells, depending on how many nodal surfaces they have. An orbital belonging to shell n has $n - 1$ nodal surfaces. For light atoms, an orbital in a higher shell always has higher energy than an orbital in a lower shell. The orbitals also have different symmetries. s orbitals are spherically symmetric around the atom. p orbitals are cylindrically symmetric, with a nodal plane passing through the atom. Purple regions in figure 2.1 are regions where the wavefunction is negative, and green regions are where it is positive. There are no $1p$ orbitals, but from shell 2 and on, there are three p orbitals per shell, one in each coordinate direction. For higher shells, there are also d and f orbitals, but they will not concern us.

Carbon is the main building block of all organic molecules. It has six electrons. Two of them sit comfortably in the $1s$ orbital. The rest have to occupy orbitals in the second shell, lying further from the nucleus and higher in energy. These four electrons are the ones involved in chemical bonding. The orbitals describing how carbon forms bonds to other atoms are not the ones describing an isolated carbon atom, but rather linear combinations

Figure 2.1: A p orbital



of these. Only the orbitals from the second shell are used, since only the electrons of the second shell are involved in bonding.

When a carbon atom binds to four other atoms, we need four hybrid orbitals. To account for this, we have to use all of the four native orbitals of shell 2. The result is called sp^3 orbitals. They each point to a corner in a tetrahedron. The sp^3 orbitals can overlap head-on with orbitals on other atoms, giving a bond that has rotational symmetry around the line of the bond. This type of bonding is called σ -bonding.

If the carbon atom binds only to three other atoms, we instead use only $2s$, $2p_x$ and $2p_y$ to form the hybrid orbitals for the bonds. The resulting sp^2 orbitals lie in the xy plane, pointing to the corners of an equilateral triangle. The p_z orbital is left in its native state, containing an electron. If an adjacent atom is also sp^2 -hybridized, the two p_z orbitals can interact, resulting in a bond that has a nodal plane containing the line of the bond. Such a bond is called a π bond.

A π bond may extend over more than two atoms. An example of this is benzene, with the chemical formula C_6H_6 . The six carbons form a regular hexagon, where each carbon also is attached to a hydrogen. All of the carbon atoms are therefore sp^2 -hybridized, and there are six p_z orbitals left over. These interact, forming six new π orbitals, shown in figure 2.2. The six π electrons will occupy the three lowest π orbitals. Molecules which have these π orbitals spread over most of the molecule are called aromatic. The name arose because most of these molecules have rather strong smells.

Finally, we must mention the hydrogen bond. This is much weaker than σ or π bonds, as it is based not upon the sharing of an electron pair, but rather on dipole-dipole interaction. If hydrogen is bound to an atom such as oxygen or nitrogen, the heavy nucleus will attract the shared electrons much more than the single proton does, leading to a dipole. If the proton is in the vicinity of another oxygen or nitrogen, the dipoles will attract each other due to Coulomb forces. A typical energy for a hydrogen bond is between 0.1 eV and 0.4 eV. Energies for the covalent σ and π bonds are typically ten to twenty times larger.

2.2 DNA bases

The DNA bases, like benzene, are built from sp^2 -hybridized atoms lying in a plane. Cytosine and thymine have six-membered rings, while the basic structure of adenosine and guanine is a five-membered ring fused to a six-membered one. Like in benzene, the p_z orbitals of the ring members combine to give π orbitals, spanning the whole molecule. The DNA bases are aromatic

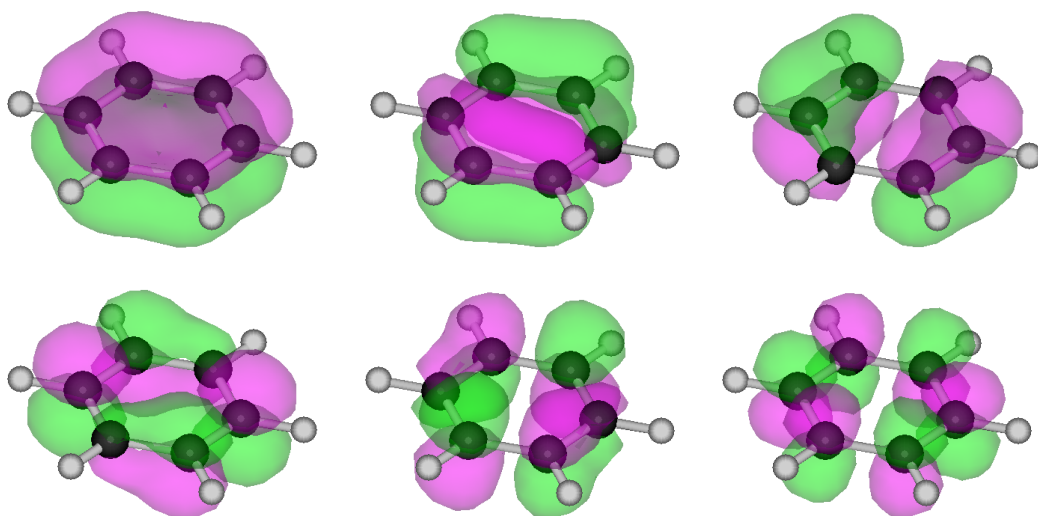


Figure 2.2: The six π orbitals of benzene

molecules. Pictures of them can be found in figures 2.3 and 2.4. In these figures, standard chemistry color-coding is used: black denotes carbon, white stands for hydrogen, red for oxygen and blue for nitrogen.

Each base is attached to a sugar molecule named deoxyribose (the 'D' in DNA). Its structure is shown in figure 2.5. Deoxyribose is a pentose, a sugar with five carbon atoms. Most sugars have as many oxygens as carbons, but deoxyribose only has four, hence the prefix 'deoxy-'. The five carbons are numbered clockwise, starting with the rightmost one in the figure. The bases attach to carbon number one. Carbon number three on one deoxyribose-base-unit then attaches to carbon number five of another unit, via a molecule of phosphoric acid. This phosphoric acid is responsible for DNA itself being acidic.

As can be seen in figures 2.3 and 2.4, guanine can associate with cytosine, forming three hydrogen bonds (the dashed lines). Likewise, adenine and thymine form two hydrogen bonds. However, trying to match guanine with thymine, or adenine with cytosine, will not work. The hydrogens are in the wrong place.

Now, we put everything together: the sugar-phosphate backbone, bases attached to it, the complementary bases associating with the first strand through hydrogen bonds, and the second backbone. The result is a DNA molecule. It is evident from figure 2.6 that the planes of the base pairs are parallel to each other. The distance from base pair to base pair is about 3.4 Å. This is short enough for the π orbitals of the base pairs to have a small overlap head-on. It would then be possible for electrons to travel the length of the DNA molecule. This has been the subject of many studies, both experimental and theoretical. In the present work, I have used a much simplified approach.

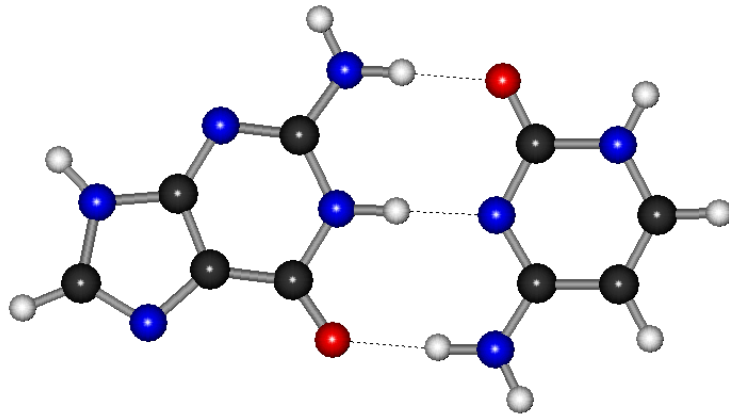


Figure 2.3: Guanine and cytosine

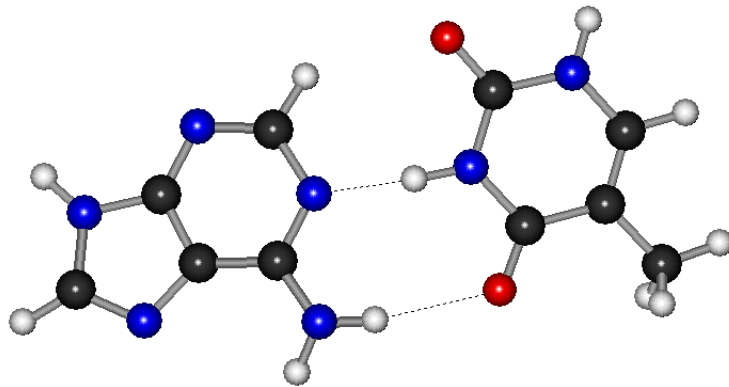


Figure 2.4: Adenine and thymine

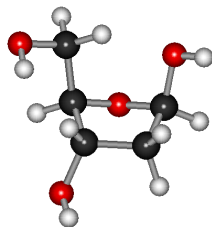


Figure 2.5: Deoxyribose

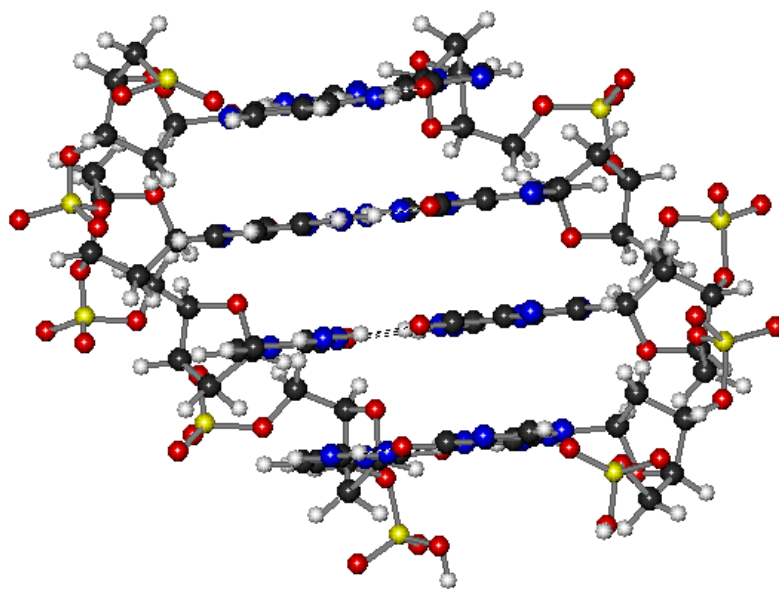


Figure 2.6: A short strand of DNA

Chapter 3

Some basic theory of mesoscopic electronics

3.1 The relation between conductance and transmittance

We will use the model system in the figure. This consists of two contacts with chemical potentials μ_1 and μ_2 respectively. Two thin leads are attached to the contacts, and to a one-dimensional conductor in the middle. The states of the electrons in the leads are denoted k_i^\pm , where $i = 1, 2$ tells which lead we are looking at, $+$ means electrons moving towards the right, and $-$ means electrons going to the left. The possibility that the conductor will transmit an electron is T . We assume that the temperature is at 0K.

Now suppose that an electron always can pass from a lead to a contact without being reflected. This means that the states k_1^+ are populated only by electrons from contact 1, since the electrons in k_1^- will not be reflected into k_1^+ . These electrons will therefore have chemical potential μ_1 . For the

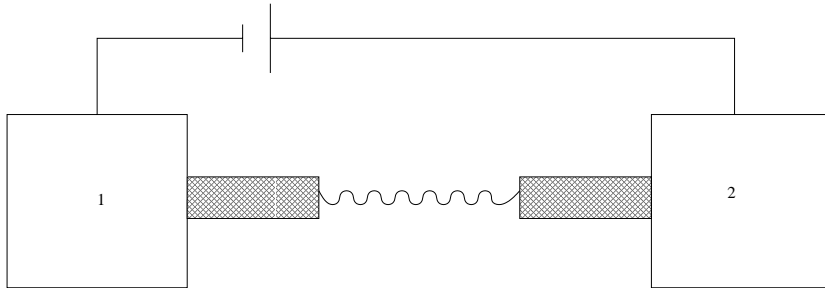


Figure 3.1: The model system

same reason, the electrons in k_2^- will have chemical potential μ_2 .

The current from contact 1 to lead 1 is then

$$I_1^+ = \frac{2e}{h}(\mu_1 - \mu_2)$$

Of this current a fraction T will pass the conductor, while a fraction $(1 - T)$ will be reflected to I_1^- :

$$I_2^+ = \frac{2e}{h}T(\mu_1 - \mu_2)$$

$$I_1^- = \frac{2e}{h}(1 - T)(\mu_1 - \mu_2)$$

The total current between the contacts becomes

$$I = I_1^+ - I_1^- = \frac{2e}{h}T(\mu_1 - \mu_2)$$

and so the conductance is

$$G = \frac{I}{(\mu_1 - \mu_2)/|e|} = \frac{2e^2}{h}T \quad (3.1)$$

From now on, we will focus on the transmittance T .

3.2 Green's functions

We want to solve a modified Schrödinger equation

$$(E - H)\Psi = S \quad (3.2)$$

where S denotes some kind of perturbation. Formally we can write

$$\Psi = (E - H)^{-1}S$$

and it is easily seen that if we know the inverse operator $(E - H)^{-1}$ we can solve the equation for any S . $(E - H)^{-1}$ is called a Green's function.

Let $G(x, x') = (E - H)^{-1}$. In one dimension we have

$$(E - H)G(x, x') = \delta(x - x')$$

So, the Green's function G can be seen as an impulse response. NB that the differential equation above has two solutions, depending on what boundary conditions we choose. Suppose in particular that $H = U_0 - \frac{\hbar^2}{2m} \frac{d^2}{dx^2}$, i. e. we are studying free electrons. Physically one expects that the unit perturbation

$\delta(x - x')$ will result in plane waves travelling away from the perturbation. The Green's function that gives this solution is called the retarded Green's function, and denoted G^R . But mathematically, an equally possible solution would be plane waves travelling towards the perturbation, and disappearing in the point $x = x'$. This solution is given by the advanced Green's function, G^A . The advanced Green's function is the hermitian conjugate of the retarded Green's function.



Figure 3.2: The interesting part of the model

Now, consider just the conductor and the leads. We will assume that the leads are much longer than the conductor, meaning that we can treat them as being semi-infinite. That way, we will not have to care about the contacts, the voltage source etc. If we know the hamiltonian matrix for the system in figure 3.2 it might seem an easy task to invert the matrix $(E - H)$ and get the Green's function of the system. But since this system is infinite, so is the matrix.

Partition the Green's function G into four parts:

$$G = \begin{pmatrix} G_m & G_{mC} \\ G_{mC} & G_C \end{pmatrix} = \begin{pmatrix} E - H_m & \tau_{mC} \\ \tau_{mC}^\dagger & E - H_C \end{pmatrix}^{-1} \quad (3.3)$$

where index m means the metal leads, C is the conductor, and mC the connection between them. It is immediately seen that

$$\begin{pmatrix} E - H_m & \tau_{mC} \\ \tau_{mC}^\dagger & E - H_C \end{pmatrix} \begin{pmatrix} G_m & G_{mC} \\ G_{mC} & G_C \end{pmatrix} = \begin{pmatrix} 1 & 0 \\ 0 & 1 \end{pmatrix}$$

$$\begin{cases} (E - H_m)G_{mC} + \tau_{mC}G_C = 0 \\ \tau_{mC}^\dagger G_{mC} + (E - H_C)G_C = 1 \end{cases}$$

$$G_{mC} = -(E - H_m)^{-1}\tau_{mC}G_C$$

$$G_C = (E - H_C - \tau_{mC}^\dagger(E - H_m)^{-1}\tau_{mC})^{-1} \quad (3.4)$$

The function $g_m = (E - H_m)^{-1}$ is the Green's function for the isolated lead. Since the lead is homogeneous, we can compute the Green's function analytically, and thus we will not have to invert an infinite matrix. $\tau_{mC}^\dagger g_m \tau_{mC}$ is called the self energy of the lead, and denoted Σ . Because the lead's Green's function comes in two varieties, the retarded and the advanced Green's function, the so does the self energy.

3.3 Self energy for a two dimensional metal lead

Suppose that we have a two dimensional metal lead, where the electrons are free to move in the x direction, while in the y direction they are confined by a well potential

$$U(y) = \begin{cases} 0 & 0 \leq y \leq d \\ \infty & y \leq 0, y \geq d \end{cases}$$

The movement of electrons in such a lead can be described by the equation

$$\left(E_s + \frac{p_x^2 + p_y^2}{2m} + U(y) \right) \Psi(x, y) = E \Psi(x, y) \quad (3.5)$$

It is easy to see that this equation is separable, and

$$\Psi(x, y) = \frac{1}{\sqrt{L}} e^{ikx} \chi(y)$$

where L denotes the normalisation length of the wave function. The equation for $\chi(y)$ is

$$\left(E_s + \frac{\hbar^2 k^2 + p_y^2}{2m} + U(y) \right) \chi(y) = E \chi(y)$$

with solutions

$$\chi_n(y) = \sin\left(\frac{n\pi y}{d}\right)$$

The different χ_n are called different transverse modes of the electrons. To find the self energy of a semi-infinite lead, we sum over the transverse modes containing electrons:

$$\Sigma^R(1, 2) = -t_m \sum_m \chi_m(y_1) e^{ik_m a} \chi_m(y_2) \quad (3.6)$$

where $k_m = \frac{\sqrt{2m(E-\varepsilon_0)}}{\hbar}$, $\varepsilon_0 = \frac{\hbar^2 n^2 \pi^2}{2md^2}$, a denotes the distance between two lattice points in the metal, and t_m is the overlap between the metal lead and the conductor. For a derivation of this, see [13], chapter 3.

3.4 The Fisher-Lee-relation

Remember that index 1 denotes the left lead, and index 2 the right. If we define the quantity

$$\Gamma_j = i(\Sigma_j^R - \Sigma_j^A)$$

where $j = 1, 2$, it can be shown that the transmittance from left to right is given by

$$T = Tr(\Gamma_2 G^R \Gamma_2 G^A) \quad (3.7)$$

where Tr denotes the trace of the matrix. This important formula is called the Fisher-Lee-relation. The proof can be found in [13]. As it requires the use of scattering matrices, I will not relate it here.

3.4.1 When is the Fisher-Lee relation applicable?

A basic requirement for the use of the above formalism is that scattering is elastic. That is, the mean free path of an electron must be much larger than the length of the conductor, so that the electron does not lose its phase during transport. It is this feature that allows us to disregard the exclusion principle. If we allow inelastic scattering, where the electrons change their energy, the exclusion principle enters the calculations in a rather complicated way that is better avoided.

Chapter 4

Tight-binding models for DNA

4.1 Generic tight-binding model

The tight-binding model deals with particles moving on a lattice. The basic assumption is that a particle in a lattice site can only move to neighbouring sites. In one dimension and using standard creation (a_i^\dagger) and annihilation (a_i) operators, this becomes

$$H = \sum_i \varepsilon_i a_i^\dagger a_i + \sum_i (t_{i,i-1} a_i^\dagger a_{i-1} + t_{i,i-1}^\dagger a_{i-1}^\dagger a_i) \quad (4.1)$$

When doing tight-binding calculations on DNA, a natural 'lattice point' is a base or base pair, and the particles moving are electron holes. The on-site energy ε_i is then the ionization potential of the base. The overlap integrals t have in the present work been treated as parameters, as has the overlap between the DNA molecule and the metal, t_m .

In the position base, the hamiltonian matrix of the tight-binding model is

$$H = \begin{pmatrix} \varepsilon_1 & t_{1,2} & 0 & 0 & \dots & \dots & \dots & 0 \\ t_{1,2}^\dagger & \varepsilon_2 & t_{2,3} & 0 & & & & \cdot \\ 0 & t_{2,3}^\dagger & \varepsilon_3 & t_{3,4} & & & & \cdot \\ 0 & 0 & t_{3,4}^\dagger & \varepsilon_4 & & & & \cdot \\ \cdot & & & & \cdot & & & \cdot \\ \cdot & & & & & \cdot & & \cdot \\ \cdot & & & & & & \cdot & \cdot \\ \cdot & & & & & & \varepsilon_{N-1} & t_{N-1,N} \\ 0 & \cdot & \cdot & \cdot & \cdot & \cdot & t_{N-1,N}^\dagger & \varepsilon_N \end{pmatrix}$$

4.2 The two-channel tunneling model

Several authors have proposed a tunneling model for hole transport in DNA: the hole is injected on a G base, then tunnels from G base to G base until it reaches a sink. The physical motivation for this is that a hole on a guanine unit has lower energy than a hole on any other DNA base, and thus a G^+ cannot oxidize any other base.

The tunneling probability decays exponentially with the distance. A possible formulation of the hole tunneling model is therefore

$$H = \sum_j \varepsilon_j a_j^\dagger a_j + \sum_j (t_G e^{-\beta n_{j,j-1}} a_j^\dagger a_{j-1} + h.c.) \quad (4.2)$$

Here, β is a decay parameter, $n_{j,j-1}$ is the number of bases between G_{j-1} and G_j , and the letters *h.c.* denotes the hermitian conjugate of the preceding term.

I have extended this model, adding the possibility that electrons are injected on a T base, and then tunnel from T base to T base until they reach the other lead. This idea was partly inspired by the paper by Yoo *et al.*, ([6]), who found that a poly(GC)-molecule is a p-type semiconductor, while a poly(AT)-molecule is an n-type semiconductor. In analogy with the G case, since a T base has the lowest electron affinity of the four DNA bases, a T^- cannot reduce any other base. I have not taken into account any interactions between the extra electrons and the electron holes. The full model thus becomes

$$\begin{aligned} H = & \sum_j \varepsilon_j a_j^\dagger a_j + \sum_i \varepsilon_i b_i^\dagger b_i + \\ & + \sum_j (t_G e^{-\beta n_{j-1,j}} a_j^\dagger a_{j-1} + h.c.) + \sum_i (t_T e^{-\beta n_{i-1,i}} b_i^\dagger b_{i-1} + h.c.) \end{aligned} \quad (4.3)$$

In this model, index i counts the T bases and index j the G bases. It is essentially a tight-binding model with variable overlap, featuring two independent species. In matrix notation, this becomes

$$H_{el} = \begin{pmatrix} \varepsilon_T & t_T e^{-\beta n_{1,2}} & 0 & \dots & \dots & 0 \\ t_T^\dagger e^{-\beta n_{1,2}} & \varepsilon_T & t_T e^{-\beta n_{2,3}} & \dots & \dots & \dots \\ 0 & t_T^\dagger e^{-\beta n_{2,3}} & \varepsilon_T & \dots & \dots & \dots \\ \dots & \dots & \dots & \dots & \dots & \dots \\ \dots & \dots & \dots & \dots & \dots & \dots \\ \dots & \dots & \dots & \dots & \varepsilon_T & t_T e^{-\beta n_{N_T-1,N_T}} \\ 0 & \dots & \dots & \dots & t_T^\dagger e^{-\beta n_{N_T-1,N_T}} & \varepsilon_T \end{pmatrix}$$

$$H_{hole} = \begin{pmatrix} \varepsilon_G & t_G e^{-\beta n_{1,2}} & 0 & \dots & \dots & 0 \\ t_G^\dagger e^{-\beta n_{1,2}} & \varepsilon_G & t_G e^{-\beta n_{2,3}} & & & \cdot \\ 0 & t_G^\dagger e^{-\beta n_{2,3}} & \varepsilon_G & & & \cdot \\ \cdot & & & \cdot & & \cdot \\ \cdot & & & & \cdot & \cdot \\ \cdot & & & & & \cdot \\ \cdot & & & & & \cdot \\ 0 & \cdot & \cdot & \dots & t_G^\dagger e^{-\beta n_{NG-1,NG}} & \varepsilon_G \end{pmatrix}$$

$$H = \begin{pmatrix} H_{el} & 0 \\ 0 & H_{hole} \end{pmatrix}$$

4.3 Parameters

For the generic tight-binding model, the parameters of the Hamiltonian are the on-site energies ε and the overlap integrals t . Following Roche ([14]), I have mostly studied t in the range $0.4 \leq t \leq 1$ eV. Semi-empirical studies of the overlap have given much smaller values ([15],[16]).

As the moving species is electron holes, the on-site energies are modeled by the ionization potentials of the isolated bases, as calculated by Sugiyama and Saito ([17]). More calculated values can be found in [16], [18], [19], and [20]. [19] also contain data on the effect of base pairing.

In the two-channel model, I have kept t fixed at 1 eV, and instead varied β . A physically realistic value would be $\beta = 0.34$ ([16]). ε_G is the same as above, but the species on the T bases is now electrons. For ε_T I therefore use a value of the electron affinity of isolated T, calculated by Colson *et al.* ([18]).

There are also certain variables associated with the self energy, see section 3.3. The width d of the lead has again been treated as a parameter, with values ranging from 0.3 to 100 nm. The overlap t_m between the leads and the DNA has been chosen from the range $0 < t_m \leq 3$ eV. The energy E of the injected electrons I have chosen as the independent variable. Finally we have the contact point between leads and DNA, denoted y . I have chosen to set $y = d/2$, meaning that the DNA attaches to the midpoint of the lead.

Chapter 5

Calculations and results

5.1 A 30 base-pair poly(dG) molecule

The more ordered a molecule is, the more delocalized its electrons become. Hence a DNA molecule where all of the base pairs are of the same kind would be expected to be a better conductor than random DNA. (A recent paper by Caetano and Schulz ([21]), however, suggests that the short-range order, introduced by base pairing, alone is sufficient for delocalization of the molecular orbitals.) It has experimentally been found that a poly(dG) molecule conducts better than a poly(dA) molecule (see for instance [6]). Consequently, most of my calculations have been performed on a DNA oligomer with 30 base pairs, all of which are GC. This means that the hamiltonian matrix is 30 by 30, and that all $\varepsilon=7.75$ eV. The number 30 was chosen to facilitate comparisons with Roche's results ([14]). Roche uses a tight-binding model for the leads as well, while I have been modeling the leads as two-dimensional waveguides with a number of different transverse modes.

Figure 5.1 shows the influence of the width of the leads. The abscissa (I'd like to avoid the term 'x-axis', since the name of the variable associated with this axis is not necessarily x) shows the electron energy E in eV, and the ordinate ('y-axis') shows the transmittance of electrons. For this series of plots we have $t_m = t = 1$ eV. The first function $T(E)$ is calculated with $d = 0.3$ nm. This value is small enough that only one transverse mode is active in the current energy interval. The transmittance function is smooth, with more or less regularly spaced resonances where $T = 1$, and an envelope which has a large maximum around $E = 7$ eV and a small local maximum around $E = 9.3$ eV. This is very similar to the result in Roche's paper. However, he finds a gap in the transmittance, between $E = 7.8$ eV and $E = 8.8$ eV, that is absent in my result.

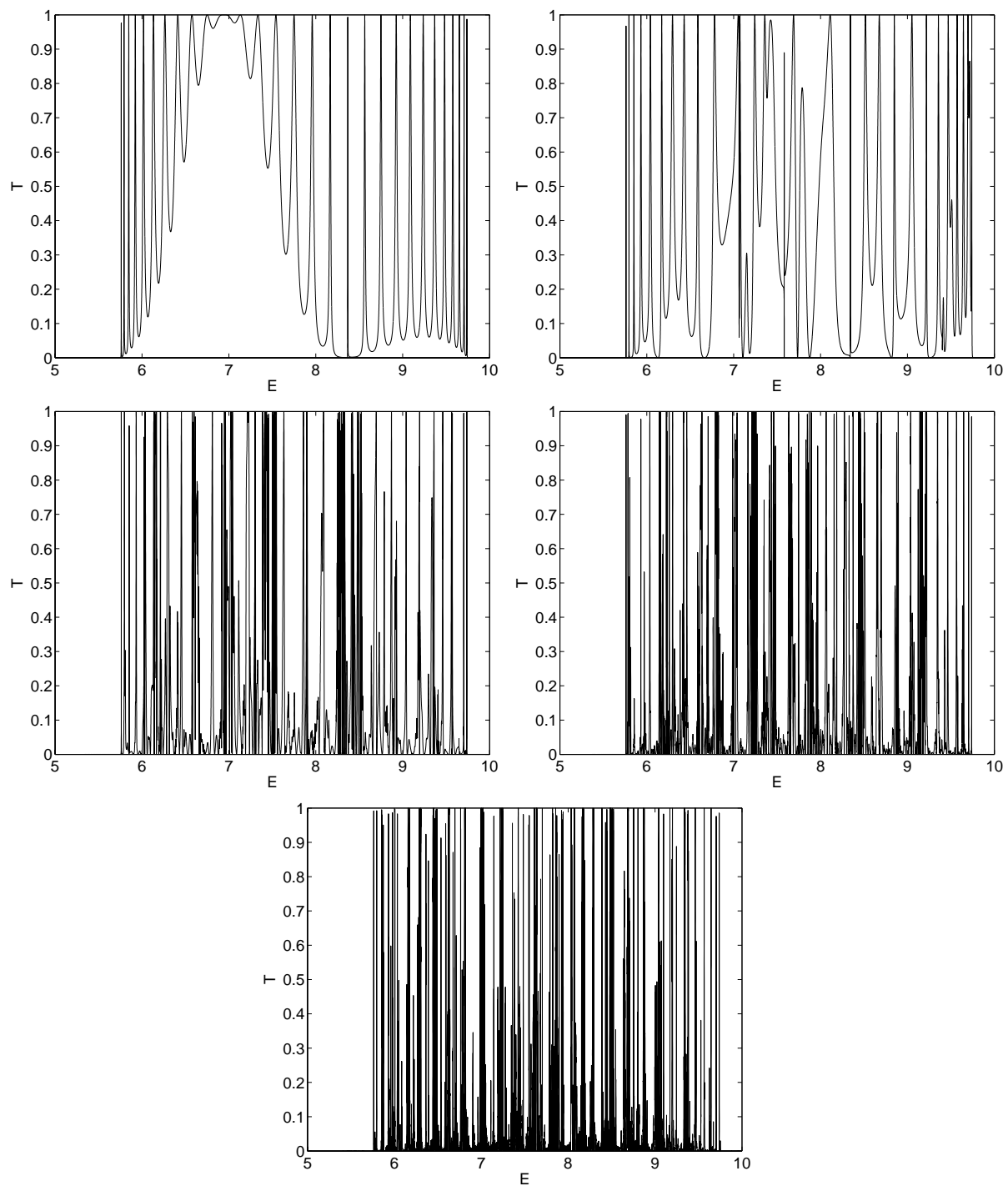


Figure 5.1: The influence of d

The second plot in figure 5.1 shows $T(E)$ for $d = 3$ nm. Now, some 10 to 15 transverse modes are active, more for higher E . The curve is more irregular than in the single-mode case, probably due to interference between the modes. This destructive interference becomes successively more pronounced in the last three plots, with $d = 25, 50$ and 100 nm respectively. For these d values, the function $T(E)$ is highly irregular and mostly close to zero, but at some energies we still find resonances where T is close to one. Hundreds of transverse modes are available, so for these widths, the lead could probably be regarded as being infinite in the y direction.

Figure 5.2 shows a selection of plots with varying t_m . The other parameters are $t = 1$ eV and $d = 50$ nm. The six subfigures have, respectively, $t_m = 0.02, 0.04, 0.1, 0.4, 1.0$ and 3.0 eV. It would appear that the dependence of transmittance on t_m is nonlinear, with a maximum at $t_m = 0.1$ eV. This trend is clarified in figure 5.3, which shows T integrated over E as a function of t_m . Several curves are shown, with different values of t . This figure reveals the maximum transmittance to be closer to $t_m = 0.3$. The nonlinear behaviour of T with t_m might be due to a crowding effect: if the contact is too easily passed, the holes might block each other's path, leading to less transmittance. Further investigation is needed to clarify if this is the reason.

As can also be seen from figure 5.3, the integral of T scales more or less linearly with t . One might expect that the effect of t is to linearly scale the transmittance. Figure 5.4 shows this to be wrong. Instead, the main effect of lowering t is to contract the whole transmission function. I have chosen the single-mode results, $d = 0.3$ nm, because they show the effect most clearly. $t_m = 1$ eV, and t goes from 0.4 eV in the first subfigure to 0.9 eV in the last. Compare also with the first subfigure of figure 5.1, where $t = 1.0$ eV.

5.2 Random DNA: 30 base-pairs from *avena sativa*

To investigate the effects of a disordered sequence, I have performed some calculations on a 30 base pair-sequence from the oat plant, *avena sativa*. The sequence in question is TAAAT TCAAT TCGCC CTATA GTGAGT CGTAT. To begin with, this was modeled only by modifying ε . I set $\varepsilon_A = 8.24$, $\varepsilon_C = 8.87$, $\varepsilon_G = 7.75$, and $\varepsilon_T = 9.14$, all values in eV. ([17]) The main effect of introducing a random sequence was to dramatically lower the number of electron energies where the system is transmitting. Again, this is most evident in the single-mode case. In figure 5.5 two plots with $t = t_m = 1.0$ eV

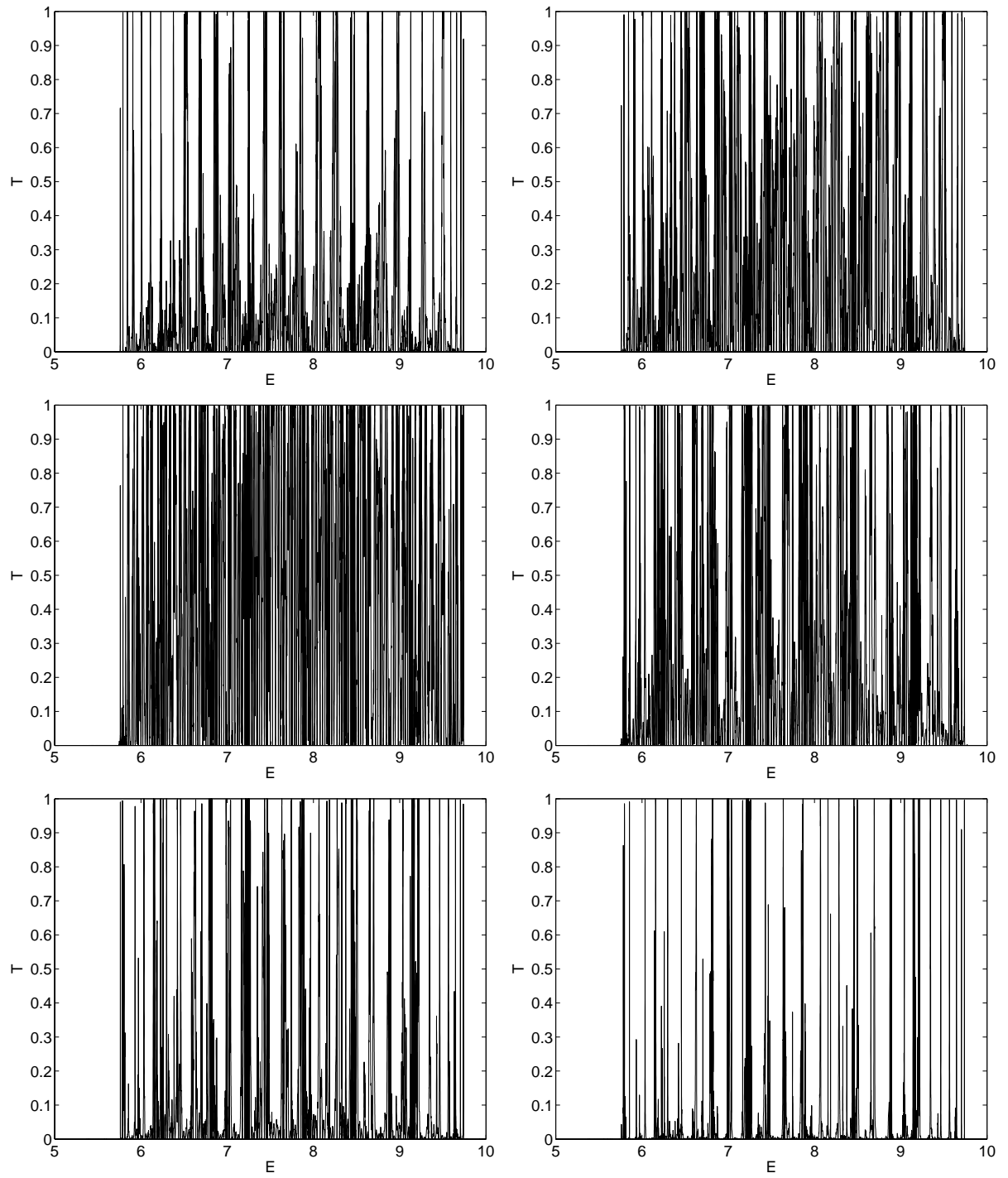


Figure 5.2: The influence of t_m

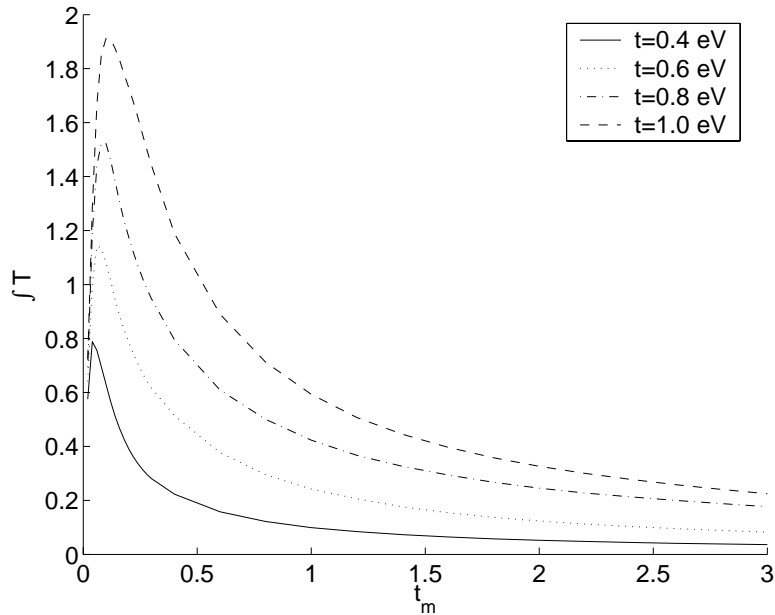


Figure 5.3: The influence of t_m , contd

are shown. The left plot has $d = 0.3$ nm, while in the right one $d = 50$ nm. The curve on the left looks a little like an envelope of the curve on the right. However, plotting both curves in the same figure shows that this is not quite true. Note for instance the resonance about 9.5 eV in the $d = 50$ nm case, that is absent in the single-mode case. These figures can be compared with Roche's ([14]) results for DNA from the λ phage.

Apart from the transmittance being decidedly less, the same trends as for a homogeneous poly(dG) molecule applies in the random sequence case.

The *avena sativa* sequence was also the one used in the two-channel model. An overview of the results can be seen in figure 5.6. Here, ε_G is still set to 7.75 eV, and $\varepsilon_T = 0.99$ eV ([18]). $t_m = t = 1$ eV, $d = 50$ nm and β and E are left as independent variables. The left figure shows what goes through the hole channel, and the right figure shows the transmittance of the electron channel. Not surprisingly, both transmit in an energy region around their respective ε . A strange thing, however, is that even though the leftmost G in the sequence is 12 base-pairs away from the left lead, there are a few energies where holes are transmitting even at a fairly high β . The effect could be due to the same phenomenon that created the peak at 9.5 eV in the right picture of figure 5.5. I suspect it is due to constructive interference among the different electron modes. At the energies where the T channel is transmitting, much fewer modes are available, which might be why the phe-

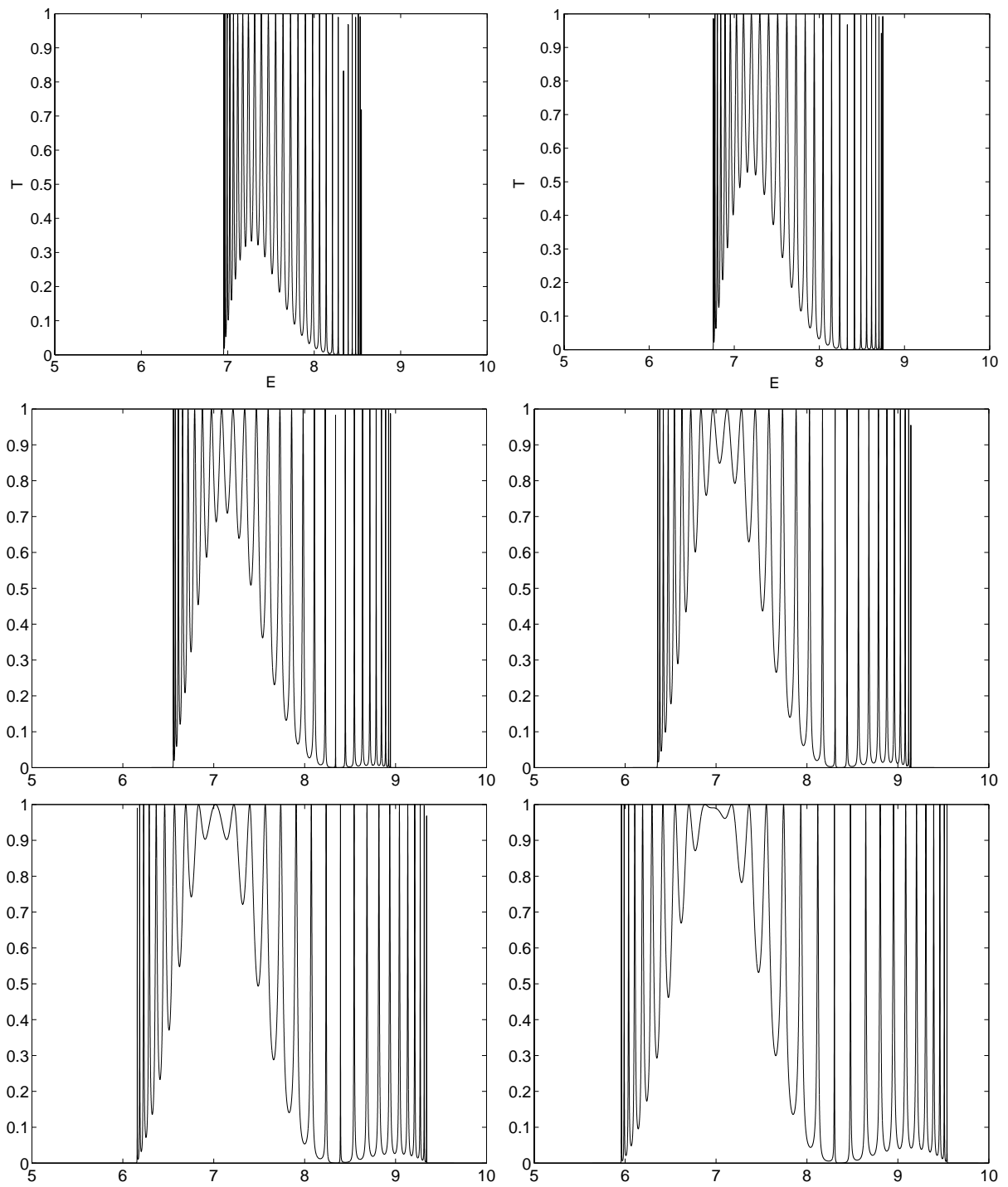


Figure 5.4: The influence of t

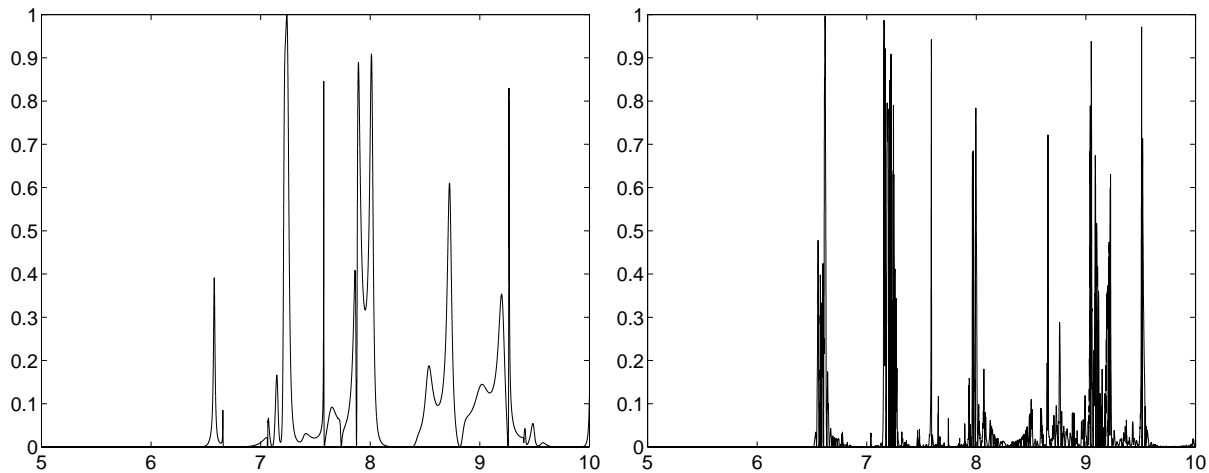


Figure 5.5: $T(E)$ for the *avena sativa* sequence

nomenon is absent there. This is pure speculation, though. More research is needed.

Figure 5.7, finally, shows the two-channel transmittance when $\beta = 0.34$. All other parameters are as above. The two peaks on the left are due to electrons, and the single peak close to $E = 8$ eV is due to holes. The sequence conducts electrons better than holes. This is only to be expected, as the T bases are regularly spaced all over the sequence, while there is a gap of 13 base-pairs between the left lead and the leftmost G.

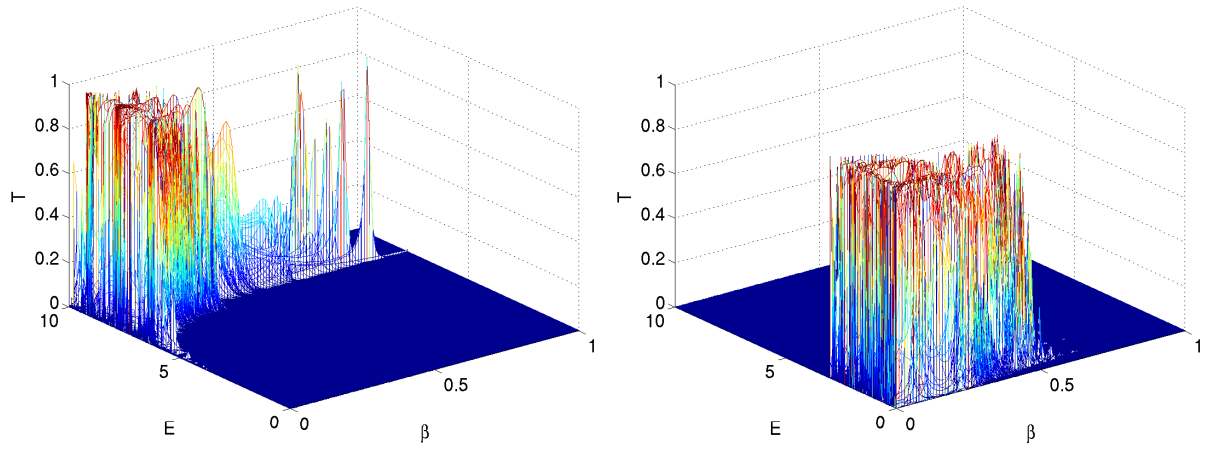


Figure 5.6: The two-channel results

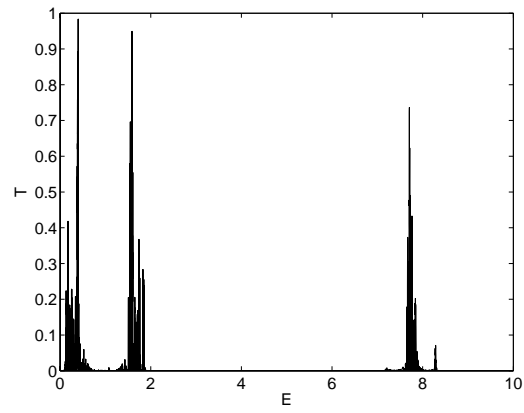


Figure 5.7: $T(E)$ at $\beta = 0.34$

Appendix A

The Matlab code used

A.1 Generic tight-binding model

A.1.1 Calculation of T

%This function gives the transmittance

```
function [T,Ntot]=transmittans3(E, t, tm)
```

```
d=50; %Width of the leads. nm
```

```
hstreck=6.582122e-16; %eVs
```

```
me=5.48579903e-4; %u
```

```
energikonversion=1.6021773e-19; %J/eV
```

```
langdkonversion=1e-9; %m/nm
```

```
viktkonversion=1.66054e-27; %kg/u
```

```
konversion=energikonversion/(langdkonversion^2*viktkonversion);
```

```
kkonv1=energikonversion*viktkonversion;
```

```
kkonv2=energikonversion;
```

```
Ntot=floor(d/(hstreck*pi)*sqrt(2*me*E/konversion)); %The number of modes
```

```
%at the given energy
```

```
if(Ntot<1)
```

```
    disp('Warning! No modes available')
```

```
end
```

```
ky=zeros(Ntot,1);
```

```
for n=1:Ntot
```

```
    ky(n)=n*pi/d;
```

```
end
```

```

Chi=zeros(Ntot,1);
y=d/2;
Chi=sin(y*ky);

epsilon_noll=hstreck^2*ky.^2*konversion/(2*me); %eV
ett=ones(size(epsilon_noll));
k=sqrt(2*me*(E*ett-epsilon_noll)*kkonv1)/(hstreck*kkonv2);

N=30; %Number of base pairs
a=2*d*langdkonversion; %The lattice distance in the lead. m
Sigma1=sparse(N,N);
Sigma2=sparse(N,N);
Sigma1(1,1)=-tm*sum(exp(i*k*a).*Chi.^2); %Coupling to lead 1
Sigma2(N,N)=-tm*sum(exp(i*k*a).*Chi.^2); %Coupling to lead 2
Gamma1=i*(Sigma1-Sigma1');
Gamma2=i*(Sigma2-Sigma2');

Hc=hamilton(N, t);
GR=inv(E*speye(N)-Hc-Sigma1-Sigma2);
T=full(trace(Gamma2*GR*Gamma1*GR'));

```

A.1.2 Calculation of the hamiltonian

H for a homogeneous molecule

%This function creates the hamilton matrix for an N base pair
 %poly(dG) molecule, with overlap integral t (eV)

```
function H = hamilton(N,t)
```

```

H=sparse(N,N);
epsilon=7.75; % eV
for k=1:N
    H(k,k)=epsilon;
    if k>1
        H(k,k-1)=-t;
        H(k-1,k)=-t;
    end
end
end

```


H for any sequence

```
%This function creates the hamiltonian matrix for any sequence.
%The sequence is entered in the vector s, according to the
%following code: A=1, C=2, G=3 and T=4. N denotes the number of
%bases according to the main program, while N2 is the length of s.
%If these are not equivalent, the program will issue a warning.
%The matrix tfakt accounts for the fact that the overlap between
%bases depends on the type of bases involved.
```

```
function H = hamiltonhavre(N,t)

s=[4 1 1 1 4 4 2 1 1 4 4 2 3 2 2 2 4 1 4 1 3 4 3 1 3 4 2 3 4 1];
N2=length(s);
H=sparse(N2,N2);
if N2 ~= N
    disp('Warning! Check number of bases!')
end

epsilon=[8.24, 8.87, 7.75, 9.14]; % eV
tfakt=[2 -1 -1 2; -1 1 1 -1; -1 1 1 -1; 2 -1 -1 2];
for k=1:N2
    H(k,k)=epsilon(s(k));
    if k>1
        H(k,k-1)=-t*tfakt(s(k),s(k-1));
        H(k-1,k)=-t*tfakt(s(k-1),s(k));
    end
end
end
```

A.2 The two-channel model

A.2.1 Calculation of T

```
%This function gives the transmittance in the two-channel case
```

```
function [T,Ntot]=transmittans32_mod2(E, beta, tG, tT, tm)

d=3; %Width of the leads, nm
hstreck=6.582122e-16; %eVs
me=5.48579903e-4; %u
```

```

energikonversion=1.6021773e-19; %J/eV
langdkonversion=1e-9; %m/nm
viktkonversion=1.66054e-27; %kg/u
konversion=energikonversion/(langdkonversion^2*viktkonversion);
kkonv1=energikonversion*viktkonversion;
kkonv2=energikonversion;

Ntot=floor(d/(hstreck*pi)*sqrt(2*me*E/konversion)); %The number of modes
    %at the given energy
if(Ntot<1)
    disp('Warning! No modes available')
end

ky=zeros(Ntot,1);
for n=1:Ntot
    ky(n)=n*pi/d;
end

Chi=zeros(Ntot,1);
y=d/2;
Chi=sin(y*ky);

epsilon_noll=hstreck^2*ky.^2*konversion/(2*me); %eV
ett=ones(size(epsilon_noll));
k=sqrt(2*me*(E*ett-epsilon_noll)*kkonv1)/(hstreck*kkonv2);

[Hc, Sigma1, Sigma2]=hamilton2_mod2(beta, tG, tT);
a=2*d*langdkonversion; %The lattice distance in the leads. m
N=size(Hc,1);
Sigma1=-tm*sum(exp(i*k*a).*Chi.^2)*Sigma1; %Coupling to lead 1
Sigma2=-tm*sum(exp(i*k*a).*Chi.^2)*Sigma2; %Coupling to lead 2
Gamma1=i*(Sigma1-Sigma1');
Gamma2=i*(Sigma2-Sigma2');

GR=inv(E*speye(N)-Hc-Sigma1-Sigma2);

T=full(trace(Gamma2*GR*Gamma1*GR'));

```

A.2.2 Calculation of the hamiltonian

%This function creates the block-diagonal hamiltonian of the
%two-channel model, for any sequence. It also creates a template
%for the self-energies Sigma1 and Sigma2, containing information
%about the number of G:s and T:s, and about the distance to the
%nearest T and G.

```
function [H, Sigma1, Sigma2] = hamilton2_mod2(beta, tG, tT)

s=[4 1 1 1 4 4 2 1 1 4 4 2 3 2 2 2 4 1 4 1 3 4 1 4 1 3 4 3 1 3];
N2=length(s);

epsilonG=7.75; %eV
epsilonT=0.99; % eV

T=zeros(size(s));
G=zeros(size(s));
Tind=0;
Gind=0;
for i1=1:N2
    if s(i1)==3
        G(i1)=1;
        Gind=Gind+1;
    end
    if s(i1)==4
        T(i1)=1;
        Tind=Tind+1;
    end
end
end

H_el=epsilonT*speye(Tind);
H_hal=epsilonG*speye(Gind);
tau=sparse(Tind,Gind);
Tdiff=zeros(1,Tind+1);
Gdiff=zeros(1,Gind+1);

Tkolla=0; Tkollb=1;
Gkolla=0; Gkollb=1;
for i2=1:N2
    Tkolla=Tkolla+1;
```

```

Gkolla=Gkolla+1;
if(G(i2))
    Gdiff(Gkollb)=Gkolla;
    Gkolla=0; Gkollb=Gkollb+1;
end
if(T(i2))
    Tdiff(Tkollb)=Tkolla;
    Tkolla=0; Tkollb=Tkollb+1;
end
end
Gdiff(Gkollb)=Gkolla+1;
Tdiff(Tkollb)=Tkolla+1;

for i3=1:Tind-1
    H_el(i3+1,i3)=-tT*exp(-beta*Tdiff(i3+1));
    H_el(i3,i3+1)=-tT*exp(-beta*Tdiff(i3+1));
end
for i4=1:Gind-1
    H_hal(i4+1,i4)=-tG*exp(-beta*Gdiff(i4+1));
    H_hal(i4,i4+1)=-tG*exp(-beta*Gdiff(i4+1));
end

H=[H_el tau; tau' H_hal];
N=size(H,1);
Sigma1=sparse(N,N);
Sigma2=sparse(N,N);
if(Tind>0)
    Sigma1(1,1)=exp(-beta*Tdiff(1));
%Coupling of electron channel to lead 1
    Sigma2(Tind,Tind)=exp(-beta*Tdiff(Tind+1));
%Coupling of electron channel to lead 2
end
if(Gind>0)
    Sigma1(Tind+1, Tind+1)=exp(-beta*Gdiff(1));
%Coupling of hole channel to lead 1
    Sigma2(N,N)=exp(-beta*Gdiff(Gind+1));
%Coupling of hole channel to lead 2
end

```

Bibliography

- [1] D D Eley and D I Spivey. Superconductivity of organic substances, part 9. *Transactions of the Faraday Society*, 58:411–415, 1962.
- [2] R G Endres, D L Cox, and R R P Singh. The quest for high-conductance DNA. *Reviews of Modern Physics*, 76:195–214, 2004.
- [3] Hans-Werner Fink and Christian Schönenberger. Electrical conduction through DNA molecules. *Nature*, 398:407–410, 1999.
- [4] Danny Porath, Alexey Bezryadin, Simon de Vries, and Cees Dekker. Direct measurement of electrical transport through DNA molecules. *Nature*, 403:635–638, 2000.
- [5] A Rakitin, P Aich, C Papadopoulos, Yu Kobzar, A S Vedeneev, J S Lee, and J M Xu. Metallic conduction through engineered DNA: DNA nanoelectronic building blocks. *Physical Review Letters*, 86(16):3670–3673, 2001.
- [6] K-H Yoo, D H Ha, J O Lee, J W Park, et al. Electrical conduction through poly(dA)-poly(dT) and poly(dG)-poly(dC) DNA molecules. *Physical Review Letters*, 87(19), 2001.
- [7] Lintao Cai, Hitoshi Tabata, and Tomoji Kawai. Self-assembled DNA networks and their electrical conductivity. *Applied Physics Letters*, 77(19):3105–3106, 2000.
- [8] A J Storm, J van Noort, S de Vries, and C Dekker. Insulating behavior for DNA molecules between nanoelectrodes at the 100 nm length scale. *Applied Physics Letters*, 79(23):3881–3883, 2001.
- [9] Y Zhang, R H Austin, J Kraeft, E C Cox, and N P Ong. Insulating behavior of λ -DNA on the micron scale. *Physical Review Letters*, 89(19), 2002.

- [10] A Yu Kasumov, M Kociak, S Guéron, B Reulet, V T Volkov, D V Klinov, and H Bouchiat. Proximity-induced superconductivity in DNA. *Science*, 291:280–282, 2000.
- [11] Tomofumi Tada, Masakazu Kondo, and Kazunari Yoshizawa. Theoretical measurements of conductance in an (AT)₁₂ DNA molecule. *ChemPhysChem*, 4:1256–1260, 2003.
- [12] T Heim, T Mélin, D Deresmes, and D Vuillaume. Localization and delocalization of charges injected in DNA. *Applied Physics Letters*, 85(13):2637–2639, 2004.
- [13] Supriyo Datta. *Electronic Transport in Mesoscopic Systems*. Cambridge Studies in Semiconductor Physics and Microelectronic Engineering. Cambridge University Press, 1995.
- [14] Stephan Roche. Sequence dependent DNA-mediated conduction. *Physical Review Letters*, 91(10), 2003.
- [15] Alexander A Voityuk, Notker Rösch, M Bixon, and Joshua Jortner. Electronic coupling for charge transfer and transport in DNA. *Journal of Physical Chemistry B*, 104:9740–9745, 2000.
- [16] Johan Olofsson and Sven Larsson. Electron hole transport in DNA. *Journal of Physical Chemistry B*, 105:10398–10406, 2001.
- [17] Hiroshi Sugiyama and Isao Saito. Theoretical studies of GG-specific photocleavage of DNA via electron transfer: Significant lowering of ionization potential and 5'-localization of HOMO of stacked GG bases in B-form DNA. *Journal of the American Chemical Society*, 118:7063–7068, 1996.
- [18] Anny-Odile Colson, Brent Besler, David M Close, and Michael D Sevilla. Ab initio molecular orbital calculations of DNA bases and their radical ions in various protonation states: Evidence of proton transfer in GC base pair radical anions. *Journal of Physical Chemistry*, 96:661–668, 1992.
- [19] Anny-Odile Colson, Brent Besler, and Michael D Sevilla. Ab initio molecular orbital calculations of DNA base pair radical ions: Effect of base pairing on proton-transfer energies, electron affinities, and ionization potentials. *Journal of Physical Chemistry*, 96:9787–9794, 1992.

- [20] Anny-Odile Colson, Brent Besler, and Michael D Sevilla. Ab initio molecular orbital calculations of DNA radical ions 4: Effect of hydration on electron affinities and ionization potentials of base pairs. *Journal of Physical Chemistry*, 97:13852–13859, 1993.
- [21] R A Caetano and P A Schulz. Double chains with base pairing: Delocalization irrespective to DNA sequencing. arXiv:cond-mat/0409245.